Eur Biophys J (1990) 18:301–307

European Biophysics Journal

Microspectrofluorimetric study of the kinetics of cellular uptake and metabolization of benzo(a)pyrene in human T 47D mammary tumor cells: evidence for cytochrome P_1450 induction

F. Sureau, L. Chinsky, M. Duquesne, A. Laigle, P.-Y. Turpin, C. Amirand, J. P. Ballini, and P. Vigny

Laboratoire de Physique et Chimie Biomoléculaire (CNRS U.A. 198), Institut Curie and Université Paris VI, 11 rue P. & M. Curie, F-75231 Paris Cedex 05, France

Received September 13, 1989/Accepted in revised form April 18, 1990

Abstract. The kinetics of penetration, activation and detoxification of benzo(a)pyrene were determined by near U.V. microspectrofluorimetric measurements on single living cells. This technique allows one to monitor the different intracellular fluorescent species present in a subcellular microvolume by using spectral decomposition of the fluorescence data. The T47-D cell line was chosen for its high capability of metabolization. The penetration involves a simple diffusion transfer through the cytoplasmic membrane of the cell, with a half-time of ~ 2 min. The metabolization process gives rise, with more than a one hour delay after intracellular incorporation of the hydrocarbon, to a rapid conversion of B(a)P into unconjugated metabolites, leading to a transient accumulation of the 3OH-B(a)P metabolite in the cell. This feature may be related to the enhancement of cytochrome P_1450 activity, induced by the B(a)P itself. The ability of the cell to increase its Cyt-P_1450 level, after exposure to B(a)P, gives indirect evidence for the presence of the Ah gene complex in the T47-D cell line.

Key words: Microspectrofluorimetry – Benzo(a)pyrene – T47-D cells – Cyt-P_1450 induction – Kinetic study

Introduction

The T 47D cell line has been isolated from pleural effusion fluid by Keydar et al. (1979), from a patient with breast carcinoma. Previous work on the metabolic pathway of benzo(a)pyrene has demonstrated that this cell line shows a high capability of metabolization for B(a)P (Selkirk and Nikbakht 1984). Moreover, the similarity of the B(a)P deoxyribonucleotide adducts observed in normal mammary epithelial cells and in human mammary carcinoma T 47D cells (Pruess-Schwartz et al. 1986) suggests that this line may provide a useful system for the study of the various aspects of polycyclic aromatic hydrocarbon (PAH) activation and detoxification in human epithelial tissues.

The activation of B(a)P is achieved by the aryl hydrocarbon hydroxylase (AHH) system of the cell. This enzymatic system catalyzes the oxidation of B(a)P to epoxide, which in turn can be converted to phenols and quinones, hydrolyzed enzymatically to dihydrodiols (DHD), or conjugated with glutathione by glutathione-SH transferase. One of these metabolites, (+)-anti-B(a)PdE:dGuo, is the major ultimate carcinogen which has been correlated with DNA adduct formation (MacNicoll et al. 1980) and the possibility of subsequent tumor formation.

Cell detoxification is achieved through further oxidation or enzymatic conjugation with glucuronic acid or sulfate, which can convert phenols and DHD to water-soluble metabolites before translocation across the cell membrane towards the culture medium (Merrick et al. 1985). Thus, the metabolism of PAH regulates the formation of ultimate carcinogens, as well as the detoxification of these agents. The relative balance of these enzyme activities plays a key role in determining the accumulation of the ultimate carcinogen in the cell and the duration of the exposure of the cell to this carcinogen.

The present report describes the kinetics of penetration, activation and detoxification of B(a)P within intact living cells by using a microspectrofluorimetry (MSF) technique, which enables one to analyze the intracellular behaviour of exogenous agents (Vigny et al. 1989; Kohen 1989; Gigli et al. 1989; Lahmy et al. 1987 and Reyftmann et al. 1986).

The main advantages of MSF are: *i)* high sensitivity (Amirand et al. 1988), comparable to radio-isotope labelling; *ii)* small volume analysis (a few $(\mu m)^3$) allowing chromophore spatial localization inside the cell; *iii)* compound identification by spectral analysis of the fluorescence; *iv)* it is a nondestructive technique which allows

Abbreviations: B(a)P, benzo(a)pyrene; PAH, polycyclic aromatic hydrocarbon; AHH, aryl hydrocarbon hydroxylase; (+)-anti-B(a)PdE, (+)-7β, 8α-dihydroxy-9α, 10α-epoxy 7,8,9,10-tetrahydrobenzo(a)pyrene; MSF, microspectrofluorimetry; DHD, dihydrodiol

Offprint requests to: F. Sureau

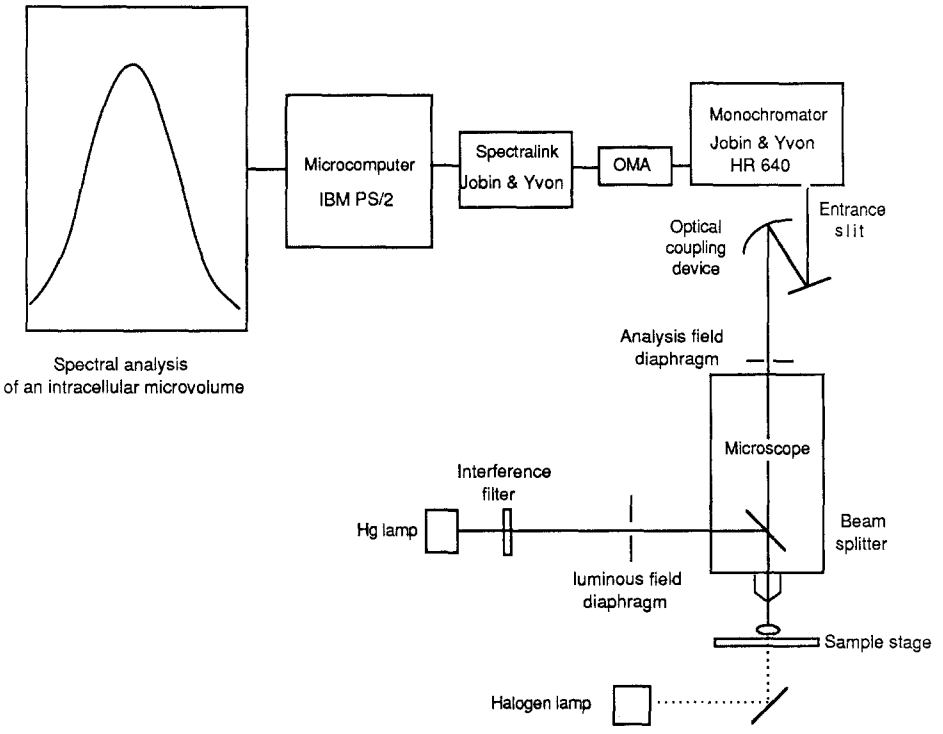

Fig. 1. Schematic block diagram of the microspectrofluorometer

studies on cells in their culture medium. Furthermore, the use of an optical multichanel analyser offers the possibility for analysis of the time evolution of the intracellular fluorescence emission on a one second time scale and thus one can monitor biological events such as the molecular modification of a drug inside living cells.

Materials and methods

Cell culture

Human T 47D mammary tumor cells were obtained from Dr. H. Magdelenat, Institut Curie, Paris. The cells were cultured as monolayers (25 cm^2 flask) in RPMI 1640 medium with 10% fœtal calf serum, L-glutamine (2 m*M*), penicillin-streptomicyn (50 units/ml, 50 µg/ml) purchased from Boehringer Mannheim. The cells were maintained in a humidified atmosphere of 95% air – 5% CO_2 at 37 °C. Confluent cultures were used for all experiments.

Preparation of B(a)P solution

A heptane solution of B(a)P was evaporated in the presence of celite 545. The treated celite was then shaken with fœtal calf serum (24 h at 37 °C). The dissolution of B(a)P in the culture medium was obtained through interaction with lipoproteins of the fœtal calf serum. The final concentration of B(a)P in the medium was adjusted to 10^{-6} M before cell incubation.

HPLC analysis of B(a)P metabolites

The B(a)P metabolites were studied from culture media and cellular extracts. 25 cm^2 of a confluent culture of T 47D cells were incubated for 24 h in 20 ml of 10^{-6} M B(a)P culture medium. The medium was then removed, and evaporated under vacuum, before resuspension in a final volume of 1 ml H_2O *Tris*. The solution was then passed through a 0.22 µm diameter filter unit (Millipore) before HPLC injection. The same protocol was applied to the cellular extracts obtained after trypsinization and sonication of the cell population. Both samples were chromatographed using a Spectroflow Kinetos analytical gradient former, equipped with a 380 Chromatem pump. The elution column was a Merck Lichrospher 100 RP-18 e, 5 µm cartridge. The elution solvent was a linear gradient increasing from 10% to 100% methanol in 45 min (flowrate: 1 ml/min). A Kontron analytical detector SFM 25 was used for fluorescence emission measurements. For optimal detection, the excitation wavelength was fixed at 365 nm and the fluorescence emission was measured at 430 nm.

Microspectrofluorimeter

The characteristics of the UV-Visible microspectrofluorimeter prototype developed in our laboratory will be extensively described in a technical paper. Briefly, the system (Fig. 1) was built around a Zeiss UMSP 80 U.V. epifluorescence microscope, optically coupled by UV reflecting mirrors to a Jobin-Yvon HR640 spectrograph. A 50 Watt Hg lamp and a 365 nm narrow band interference filter (2 nm width) were used for the excitation of B(a)P

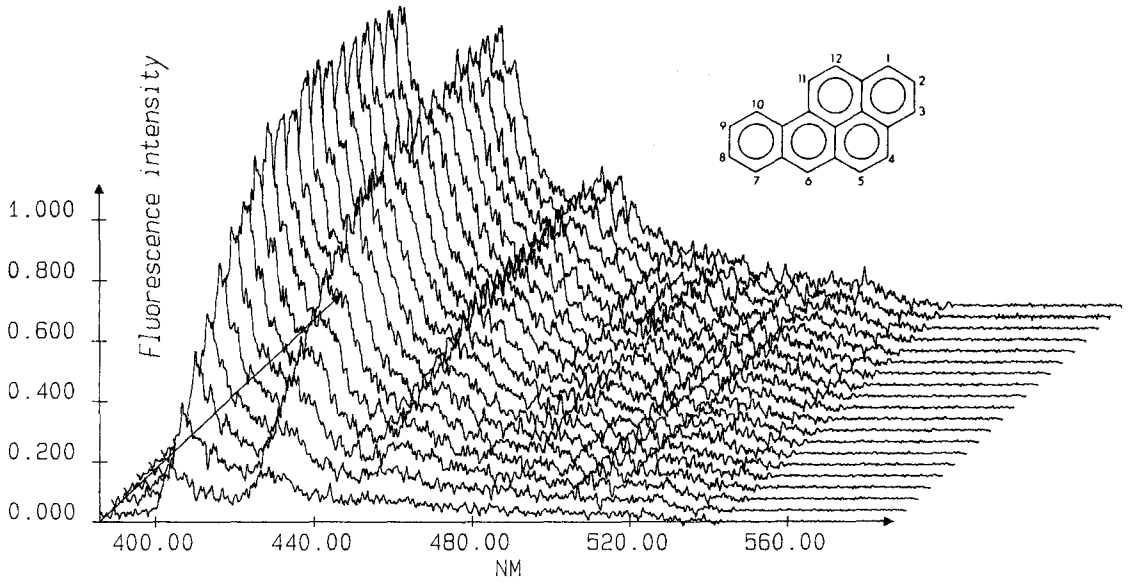

Fig. 2. Spectroscopic visualization of the cellular uptake of benzo(a)pyrene in a single human T 47D mammary tumor cell after incubation with a 10^{-6} M B(a)P solution. The fluorescence signal arises from a 2 μm diameter cytoplasmic area through a ×100 objective. Acquisition parameters: excitation wavelength = 365 nm, excitation power = 0.1 μW, acquisition time = 10 s per spectrum, delay between two spectra = 30 s

and its metabolites. A luminous field diaphragm was used in the excitation path to reduce the illuminated area to a circular spot of 6 μm in diameter. In order to avoid any photobleaching of the various fluorescent species during the experiments (Benson et al. 1985), the excitation power was reduced, by the use of optical density filters, to 0.1 μW for a typical illuminated circular area of 4 μm in diameter (for this area the photobleaching begins to be detectable for 1 μW power of excitation on a minute time scale). With an epifluorescence system, the measurement of the fluorescence signal is at 180° to the excitation beam: this generally enforces the use of a high pass band filter to prevent reflection of the excitation beam towards the emission path. In our experiments, the low intensity of the excitation beam along with the use of analysis field diaphragms (1 to 4 μm in diameter) and the good rejection of the stray light performed by the monochromator allowed us to work without a filter in the emission path. Thus it is not necessary to correct the spectra for the pass band filter transmission. The fluorescence spectra were recorded in the 380–550 nm region on a 1024 diode intensified optical multichannel analyzer (Princeton Instruments) with a resolution of 0.25 nm/diode. Data were stored and processed on a 80286 IBM PS/2 microcomputer using the Jobin-Yvon "Enhanced Prism" software.

MSF cellular experiments

Two days before the MSF studies, cells were grown on quartz plates in order to avoid any possible fluorescence from the plastic or glass support during analysis with near UV excitation. Cellular fluorescence spectra were obtained with a ×100 Zeiss Ultrafluar objective (N.A. = 1.32). The quartz plates were disposed on the microscope stage in 100 mm thermostated Petri dishes, filled with 5 ml of culture medium. The objective was immersed in the culture medium and a circular area of 1 to 4 μm in diameter was analyzed in the cytoplasmic region by interposing a field diaphragm within the microscope in the emission pathway. Accumulation of each spectrum proceeded for 10 to 30 s.

Cellular uptake

B(a)P is non-covalently associated with calf serum lipoproteins (see above) as a physiological mode of presentation of the carcinogen to the cells (Avigan 1959). The incubation was directly achieved on the microscope stage: the cell culture medium was removed and replaced with 5 ml of medium with B(a)P. The penetration was immediately observed by automatic sequential recording of the fluorescence spectra arising from the same single cell.

Cellular metabolism

For the metabolization studies, incubation with B(a)P proceeded for 10 min (this time was necessary to reach a stabilization of the drug concentration in the cell). The cells were then resuspended in 5 ml of fresh medium in order to avoid continuous influx of the parent compound into the cells. The metabolization process was then monitored by the spectral modifications of the fluorescence emission ($\lambda_{exc} = 365$ nm). Kinetic data were obtained after a linear decomposition of the experimental fluorescence spectra, using a set of model spectra (i.e. those of B(a)P and its metabolites) previously recorded under the same experimental conditions from the HPLC fractions collected from cellular extracts. The program is based on a least squares method (following Salmon et al. (1988)). The procedure involves a matrix analysis includ-

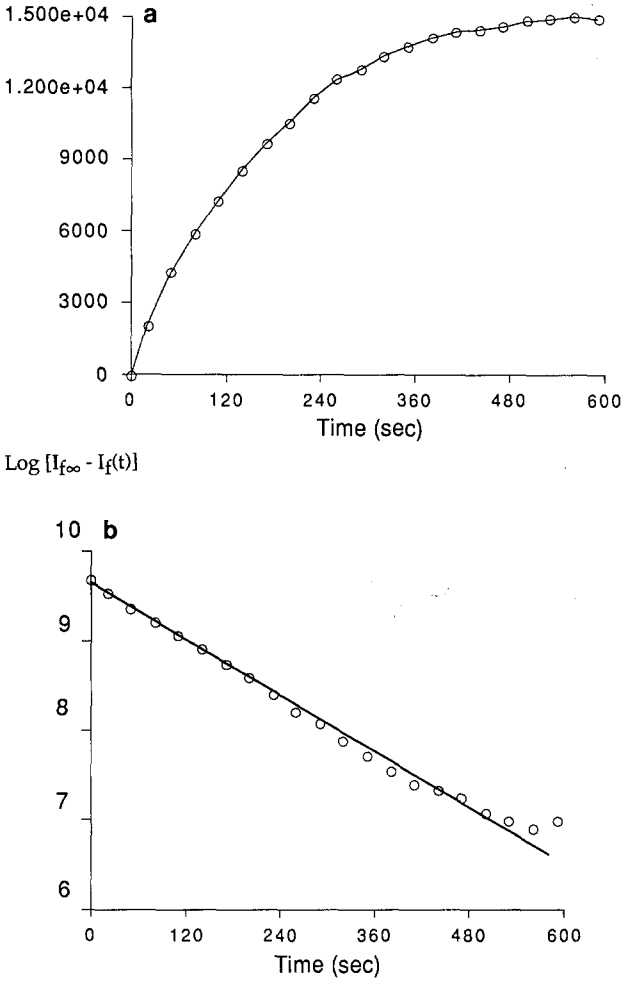

Fig. 3a, b. Kinetic profile of the cellular uptake of B(a)P obtained at 37 °C: **a** integrated fluorescence of each spectrum versus time of incubation: $t_{1/2} \sim 2$ min. **b** Linear representation characteristic of first-order kinetics: rate constant $\sim 0.38\ min^{-1}$

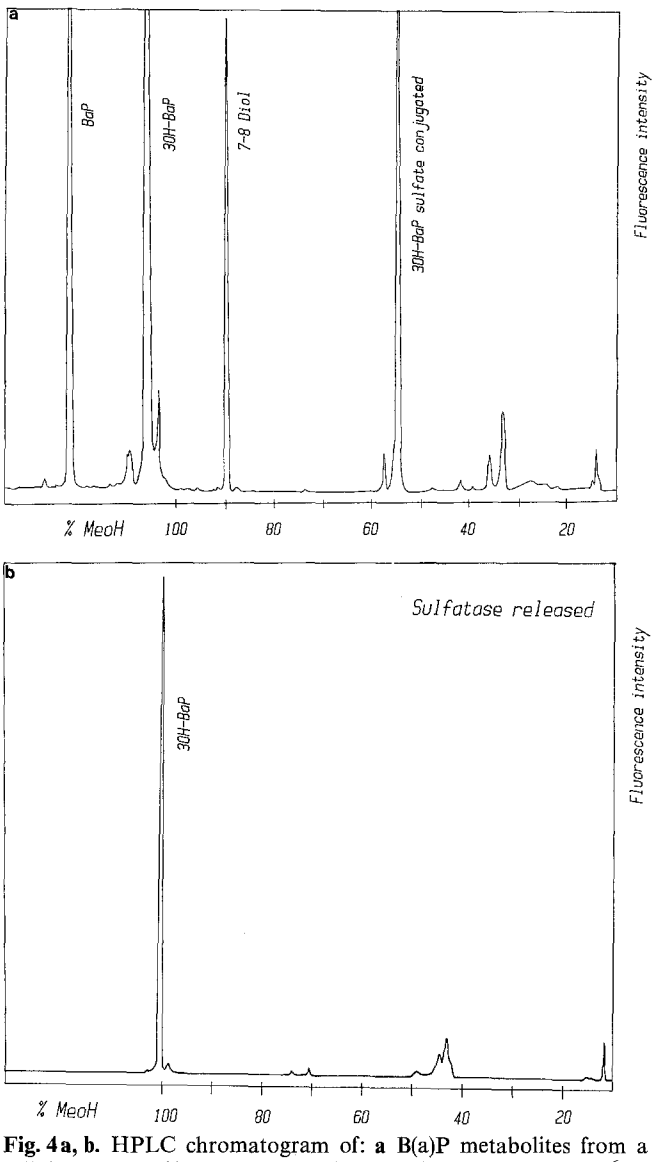

Fig. 4a, b. HPLC chromatogram of: **a** B(a)P metabolites from a cellular extract of human T 47D cells treated for 24 h with a 10^{-6} M B(a)P solution. **b** 3OH-B(a)P sulfate conjugated fraction after aryl sulfatase digestion: hydrolysis was performed at 37 °C for 2 h in a 250 µl vol. of sodium acetate buffer (0.1 M, pH 5.0) containing 10 units sulfatase activity. Fluorescence detection: $\lambda_{exc} = 365$ nm, $\lambda_{em} = 430$ nm

ing all the reference spectra and gives the coefficients of the linear combination which minimize the sum (over the 1024 channels) of the quadratic deviation between the experimental and the calculated spectra. The quality of the curve fittings are measured by a correlation coefficient, R, which is derived from the standard deviation.

Results and discussion

Cellular uptake

The time-dependent increase of the intracellular amount of B(a)P was monitored by the evolution of the intensity of the B(a)P fluorescence emission spectra arising from a cytoplasmic area of 2 µm in diameter (Fig. 2). The values of the integrated fluorescence (from 400 to 500 nm) obtained for each spectrum were plotted versus incubation time (Fig. 3a). The cellular uptake of B(a)P reaches a plateau after 10 min of incubation. The uptake profile is mono-exponential (Fig. 3b), with a half time of 2 min ± 0.2. Intercellular variations of the final concentration of intracellular B(a)P have been observed, but the uptake half-time (or the rate constant) remains the same for the different cells. If one assumes that the saturation observed after 10 min of incubation corresponds to a predetermined number (N_0) of available intracellular lipophilic sites for B(a)P, then the number of occupied sites at time t [$N(t)$] can be described by the following first-order equation:

$$dN(t)/dt = -k(N_0 - N(t)),$$

assuming that the extracellular concentration remains unchanged during the penetration process.

Thus a linear representation would be (Fig. 3b):

$$\mathrm{Ln}(N_0 - N(t)) = -kt, \quad \text{or} \quad \mathrm{Ln}(I_{f\infty} - I_f(t)) = -kt,$$

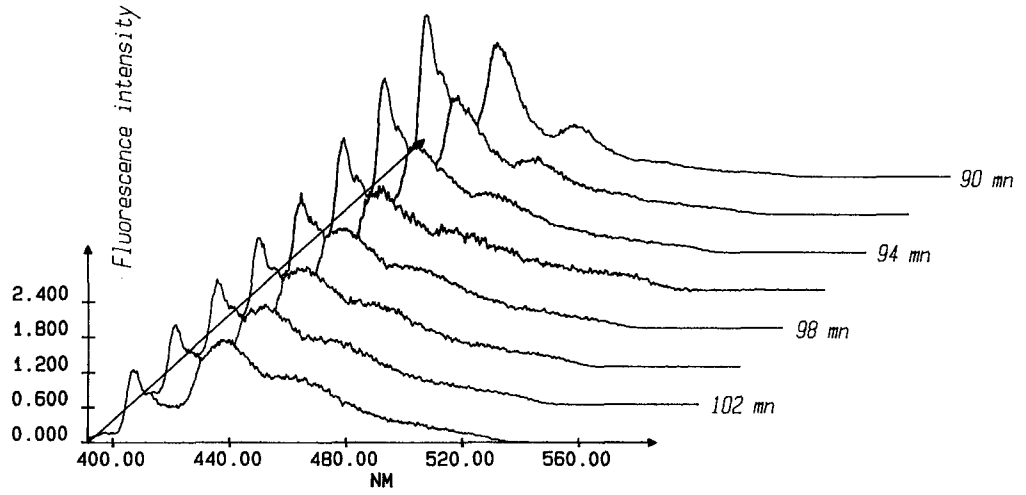

Fig. 5. Spectroscopic visualization of the intracellular conversion of B(a)P into 3OH-B(a)P, between 90 min and 104 min after a 10 min pulse of incubation with 10^{-6} M B(a)P. The fluorescence signal arises from a cytoplasmic circular area of 4 μm in diameter. Acquisition parameters: same as in Fig. 1 except delay between two spectra = 2 min

where I_f is the integrated intensity of fluorescence and k the rate constant of penetration.

These results are in agreement with those obtained by Plant et al. (1985) using digital fluorescence imaging microscopy. These authors suggested that B(a)P uptake is a simple partitioning phenomenon controlled by the relative lipoprotein content of the extracellular donor and of the cells.

Cellular metabolization

Using [^{3}H] B(a)P, Merrick et al. (1985) have shown that a confluent culture of T 47D cells metabolizes 95% of B(a)P (1 μg/ml) in 24 h. 3OH-B(a)P (unconjugated or sulfate conjugated), 7–8 diol and 9–10 diol, quinones, tetrols, and triols were identified as the major metabolites of B(a)P in the cells. The MSF analysis described here is quite different from the preceding study in its principle, since it involves the specificity of the absorption and emission characteristics of each species present in the mixture. Thus it becomes possible to favor the observation of one particular species by a judicious choice of the excitation wavelength.

In order to determine which metabolites can contribute to the total fluorescence measured during MSF experiments, HPLC profiles of the culture media and of cellular extracts were performed, using fluorescence detection (see Materials and methods). Under these conditions, tetrols, triols, 3OH-B(a)P (unconjugated, sulfate conjugated, and glucuronic-acid conjugated), and 7–8 diol-B(a)P were the major fluorescent metabolites observed, with the parent B(a)P, in the culture medium. The HPLC profiles of the metabolites obtained from the cellular extracts gave the same results, except for the lack of low polar metabolites which were more quickly released from the cell towards the extracellular medium (Fig. 4a). Each metabolite was directly identified according to its fluorescence excitation and emission spectra known from the literature (McCaustland et al. 1976), except for the sulfate conjugated 3OH-B(a)P, which was identified in a second HPLC measurement after digestion by aryl-sulfatase (Fig. 4b).

Figure 5 shows a typical time evolution of the fluorescence emission spectrum (from a 4 μm diameter circular cytoplasmic area) obtained on single cells during the metabolization phase. To protect cells from a long illumination which might affect the integrity of th cell, each spectrum was collected on a diffeent cell from the same sample. The relative contributions of the fluorescence of B(a)P and of its major metabolites were then calculated for all the MSF spectra by numerical decomposition (see Materials and methods) of the fluorescence emission (Fig. 6). The percentage of fluorescence contribution of a given component to the total fluorescence (integrated fluorescence from 400 to 500 nm) is then expressed and plotted versus time, between the initial 10 min incubation and the various times of measurement (Fig. 7). Though each data point has been measured on a different cell, a rather weak dispersion is observed on the kinetic profile. This is not the case in similar experiments made using cell cultures before confluence (data not shown). The determination of the intracellular concentration of each component, according to the fluorescence emission intensity, is not possible since the absorption coefficient and quantum yield determined "in vitro" in solution might be no longer valid in the complex "in vivo" cell environment. Moreover, it is quite impossible to take into account any fractional absorption which may occur in the cell, and consequently to make a real quantitative estimation.

Though a 10 min incubation was sufficient to reach the plateau of the intracellular incorporation of B(a)P (see Fig. 3a), the metabolization efficiency is almost negligible during the first 90 min as the fluorescence intensity of B(a)P is quite stable. Moreover, the very weak contribution of the metabolite species to the intracellular fluorescence emission observed during this period (Fig. 7B), suggests that the metabolic activation phase of B(a)P is the rate limiting step of the cell detoxification process: the conjugation step of the primary metabolites and the sub-

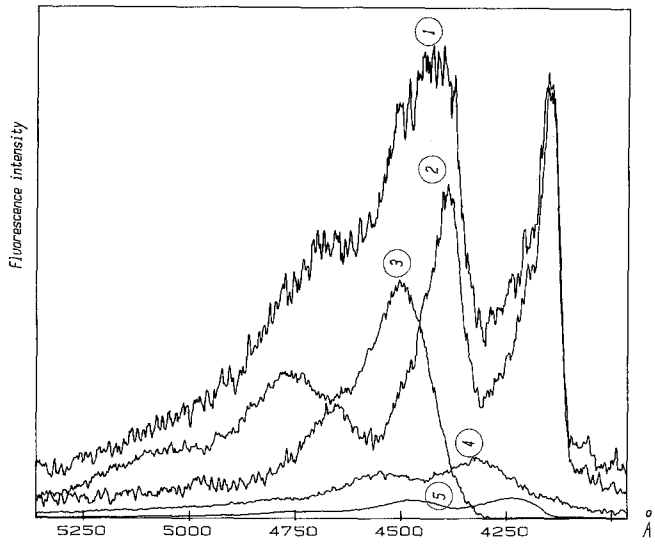

Fig. 6. Resolution of the intracellular spectrum (1) of a T 47D cell treated with 10^{-6} M B(a)P into: B(a)P (2); 3OH-B(a)P (3); 3OH-B(a)P conjugated to glucuronic acid (4) and 3OH-B(a)P conjugated to sulfate (5). An estimation of the goodness of fit between the experimental and calculated spectra obtained after numerical decomposition is given by a correlation coefficient R which is always >0.99

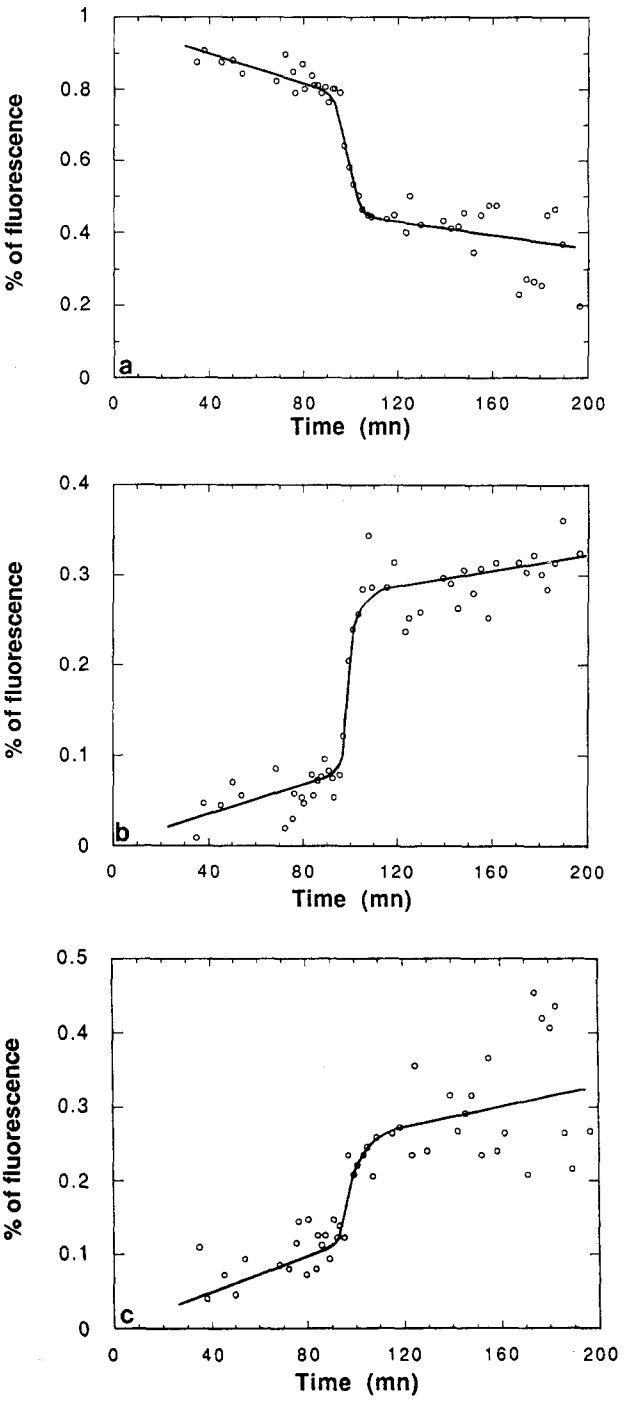

Fig. 7a–c. Relative contributions of **a** B(a)P, **b** 3OH-B(a)P and **c** conjugated forms of 3OH-B(a)P to the intracellular fluorescence spectrum recorded during the metabolization process on a 4 μm diameter circular area in the cytoplasmic region of a single cell. The origin of the x axis corresponds to the initial pulse of incubation with B(a)P. Each data point is collected from a different cell within the same sample

sequent release of water soluble metabolites is faster than the activation step produced by the cytochrome P_1450 mono-oxygenase. Then the metabolization rate suddenly increased (30-fold): one can observe a rapid conversion (in about 10 min) of B(a)P into 3OH-B(a)P (with subsequent sulfate and glucuronic acid conjugation of this phenol) leading to a new equilibrium steady state between the parent compound and the primary metabolite present in the cell. Thus the extracellular release of the primary metabolite after conjugation becomes the rate limiting step of the detoxification process.

Interpretation of this sharp feature must be related to previous biochemical work in which authors have provided:

i) evidence for AHH and Cyt-P_1450 mRNA induction after binding of B(a)P to a soluble cytoplasmic protein (namely the Ah receptor) in hepatic cytosols of various mammalian species (Denison and Wilkinson 1985; Okey et al. 1984; Fernandez et al. 1988).

ii) evidence for the presence of the Ah receptor in human T 47D mammary tumor cells (Pasanen et al. 1988; Harris et al. 1989).

The best-established function of this receptor is the regulation of Cyt-P_1450 and other enzymes associated with the Ah gene complex (Nebert et al. 1981). Thus the enhancement of the metabolization rate observed after 90 min should be a direct consequence of the induction of the enzymatic system by the B(a)P itself. Moreover the time evolution and the amplitude of the induction process observed are in agreement with previous observations (Gonzalez et al. 1984): 3 h after the treatment of C57BL/6N mice with 3-methylcholanthrene, the transcriptional rate of the mouse liver microsome Cyt-P_1450 was increased 20-fold above the control value. An important intracellular accumulation of unconjugated metabolites is the main consequence of this induction process.

These results are of biological importance, since the ability of an organism to increase its Cyt-P_1450 level in response to exogenous agents will lead to an increased ability to metabolize a PAH type carcinogen into an ultimate carcinogen.

Hence the possibility to analyze the ability of a tissue to increase its Cyt-$P_1$450 level in response to exogenous agents is of a great interest to understand the organ-specificity of cancer as well as the genetic predisposition of individuals to cancer.

This method enables one to study, within single living cells, the biological response to the induction process of the Ah gene complex, related to the binding of various agonists to the cytosolic Ah receptor. From this point of view, microspectrofluorometry appears as one of the most relevant techniques to approach molecular processes inside living cells. It allows rapid and sensitive observations, a high spatial resolution and a selective detection among the various intracellular fluorescent species.

Acknowledgements. We thank Prof. M. Manfait and Dr. J. F. Angiboust of the Laboratoire de Spectroscopie Biomoléculaire, UER de Pharmacie, Reims, France, for their help in initiating our microspectrofluorimetric experiments and for helpful discussions.

References

Amirand C, Vigny P, Moysan A, Ballini JP, Angiboust JF, Manfait M (1988) Improvement in the detection of very weak fluorescences from biological molecules by use of microspectrofluorometry. In: Schmid ED (ed) Spectroscopy of biological molecules – new advances. Wiley, New York, pp 459–462

Avigan J (1959) The interaction between carcinogenic hydrocarbons and serum lipoproteins. Cancer Res 19:831–833

Benson DM, Bryan J, Plant AL, Gotto AM, Smith LC (1985) Digital fluorescence imaging microscopy: heterogeneity of photobleaching rate constants in individual cells. J Cell Biol 100:1309–1323

Denison MS, Wilkinson CF (1985) Identification of the Ah receptor in selected mammalian species and induction of the aryl hydrocarbon hydroxylase. Eur J Biochem 147:129–435

Fernandez N, Roy M, Lesca P (1988) Binding characteristics of Ah receptor from rats and mice before and after separation from hepatic cytosols. Eur J Biochem 172:585–592

Gigli M, Rasoanaivo TWD, Millot JM, Jeannesson P, Rizzo V, Jardillier JC, Arcamone F, Manfait M (1989) Correlation between growth and intranuclear doxorubicin and 4'-iodoxorubicin quantitated in living K562 cells by microspectrofluorometry. Cancer Res 49:560–564

Gonzalez FJ, Tukey RH, Nebert DW (1984) Structural gene products of the Ah locus. Mol Pharmacol 26:117–121

Harris M, Piskorska-Pliszczynska J, Zacharewski T, Romkes M, Safe S (1989) Structure-dependant induction of the aryl hydrocarbon hydroxylase in human breast cancer cell lines and characterization of the Ah receptor. Cancer Res 49:4531–4535

Keydar I, Chen L, Karby S, Weiss FR, Yang SK, Gelboin HV (1979) Establishment and characterization of a cell line of human breast carcinoma origin. Eur J Cancer 15:659–670

Kohen E (ed) (1989) Microspectrofluorimetry of living cells. Academic Press, New York (in press)

Lahmy S, Salmon JM, Viallet P (1987) Microspectrofluorometric comparison of Benzo(a)pyrene and Dibenzo(c,h)acridine metabolism in single living 3T3 fibroblast. J Histochem Cytochem 35:197–201

McCaustland DJ, Fisher DL, Kolwyck KC, Duncan WP, Wiley JC, Menon CS, Engel JF, Selkirk JK, Roller P (1976) Polycyclic aromatic hydrocarbon derivatives: synthesis and physico-chemical characterization. In: Freudenthal RI, Jones P (eds) Carcinogenesis, vol 1. Raven Press, New York, pp 349–412

MacNicoll AD, Easty GC, Neville AM, Grover PL, Sims P (1980) Metabolism and activation of carcinogenic polycyclic hydrocarbons by human mammary cells. Biochem Biophys Res Commun 95:1599–1606

Merrick BA, Mansfield BK, Nikbakht PA, Selkirk JK (1985) Benzo(a)pyrene metabolism in human T 47D mammary tumor cells: evidence for sulfate conjugation and translocation of reactive metabolites across cell membranes. Cancer Lett 29:139–150

Nebert DW, Eisen HJ, Negishi M, Lang M, Hjelmeland LM, Okey AB (1981) Genetic mechanisms controlling the induction of polysubstrate monooxygenase (P-450) activities. Annu Rev Pharmacol Toxicol 21:431–462

Okey AB, Dubé AW, Vella LM (1984) Binding of Benzo(a)pyrene and Dibenzo(a,h)anthracene to the Ah receptor in mouse and rate hepatic cytosols. Cancer Res 44:1426–1432

Pasanen M, Stacey S, Lykkesfeldt A, Briand P, Hines R, Autrup H (1988) Induction of cytochrome P-450IA1 gene expression in human breast tumor cell lines. Chem Biol Interact 66:223–232

Plant AL, Benson DM, Smith LC (1985) Cellular uptake and intracellular localization of Benzo(a)pyrene by digital imaging microscopy. J Cell Biol 100:1295–1308

Pruess-Schwartz D, Baird WM, Nikbakht PA, Merrick BA, Selkirk JK (1986) Benzo(a)pyrene: DNA adduct formation in normal human mammary epithelial cell cultures and the human mammary carcinoma T 47D cell line. Cancer Res 46:2697–2702

Reyftmann JP, Kohen E, Morliere P, Santus R, Kohen C, Mangel WF, Dubertret L, Hirschberg JG (1986) A microspectrofluorometric study of prophyrin-photosensitized single living cells. Photochem Photobiol 44:461–469

Salmon JM, Vigo J, Viallet P (1988) Resolution of complex fluorescence spectra recorded on single unpigmented living cells using a computerized method. Cytometry 9:25–32

Selkirk JK, Nikbakht A (1984) Metabolism and macromolecular binding of benzo(a)pyrene to normal mammary epithelial cells and human mammary tumor lines T 47D, MCF-7 and HBL-100. Proc Am Assoc Cancer Res 25:121

Vigny P, Amirand C, Ballini JP, Chinsky L, Duquesne M, Laigle A, Manfait M, Sureau F, Turpin PY (1989) Microspectrofluorometry of single lining cells. In: Bertoluzza A (ed) Spectroscopy of biological molecules-state of the art. Esculapio, Bologna, pp 345–348